13th World Conference on Earthquake Engineering
Vancouver, B.C., Canada
August 1-6, 2004
Paper No. 1869

DYNAMIC INFLUENCE OF ADJACENT STRUCTURES ON PILE FOUNDATION BASED ON FORCED VIBRATION TESTS AND EARTHQUAKE OBSERVATION

Yoshio IKEDA[1], Yukio SHIMOMURA[2], Masataka NAKAMURA[3], Osamu HANEDA[4], Toshiaki ARAI[5]

SUMMARY

The purposes of our experiment are to obtain fundamental knowledge of the cross interaction among five mock-up pile foundation models and to confirm the dynamic soil property near the models under aging phenomena. Simulation analysis is conducted by the flexible volume method that takes the cross interaction of multiple foundation models into account. The soil model is assumed to be in accordance with the 3-dimensional thin layer approach. Analysis of seismic records is also carried out by the above method. To compare with the seismic records of multiple foundations and ground points, it is necessary for the simulation analysis to superpose response obtained by three components of earthquake input motions.

INTRODUCTION

After the 1985 Hanshin-Awaji Earthquake, researchers have carried out the experiments related to dynamic soil-pile interaction with soil nonlinearity [1], [2]. Nonlinear earthquake response analysis methods for pile foundation models have been presented [3], [4]. However, in these studies, only single pile foundation has been treated.

The purposes of the present paper are to grasp the basic information relating to the cross interaction among different multiple foundations [5] and to confirm the effect of secular change of the soil neighboring models on the dynamic characteristics of the foundations. The types of models are three piled foundations, an embedded and an embedded raft foundation. An identification analysis is carried out to obtain the most appropriate soil profile underneath the foundations. In this analysis, impedance functions and resonance curves obtained by forced vibration tests are compared with those by analysis. Using the soil profile, simulation analysis of multiple foundations is conducted by the flexible volume method. In

[1] Senior Engineer, Nuclear Facilities Department, Taisei Corporation, Japan.
[2] Professor, Department of Construction, Junior College of Nihon University, Japan.
[3] Assistant, Dept. of Civil Engineering, College of Science and Technology, Nihon University, Japan.
[4] Graduate Student, College of Science and Technology, Nihon University, Japan.
[5] Researcher, Research Institute, Nishimatsu Construction Co. Ltd., Japan.

the flexible volume method, the cross interaction of the models has been taken into account, and the soil is treated by the 3-dimentional thin layer method. Analysis of the seismic records of the multiple foundations and ground points is also carried out. In this analysis, we examine whether the cross interaction among foundation models affects earthquake responses.

DYNAMIC BEHAVIOR OF SOIL AND FOUNDATION

Displacement resonance curves of experimental results

Table 1 shows the titles, exciting directions, exciting force levels and conditions of the added weight at each test case. Displacement resonance curves in each exciting direction at the upper surface of the foundation model are illustrated in Fig. 1, where the added weight is included or excluded. Despite the added weight condition, amplifications of the displacement resonance curves increase and the resonance frequencies reduce in the large and medium exciting force levels. Due to the exciting schedule of the test, there is little difference between the resonance curves of the medium and large exciting force levels. Considering the added weight, reduction in the resonance frequencies and a decrease in the equivalent damping constant are observed. During the large exciting force level, no separation between the piles and the adjacent soil can be found by visual observation.

Table 1 Test information

Test name	Exciting direction	Exciting force level	Added weight
NXS	x	Small	-
NXM	x	Medium	-
NXL	x	Large	-
EXS	x	Small	○
EXM	x	Medium	○
EXL	x	Large	○

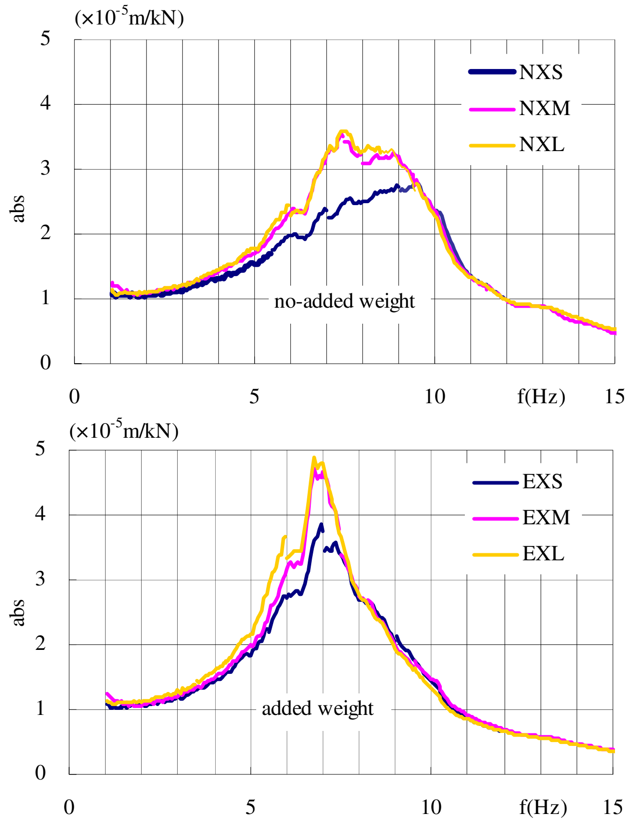

Fig. 1 Comparison of displacement resonance curves of each exciting force level at upper surface of foundation

Resonance curves of simulation analyses

The soil properties adopted in the simulation analyses are defined by the frequency-sweep test results that have a little effect on the nonlinearity of the soil around the foundation models. The final soil property shown in Fig. 2, that is, the modified analysis Case C, is obtained by comparing the results of the predicted analyses (Case 1-3). Fig. 3 displays the displacement resonance curves at the top surface of the excited foundation model with and without the added weight. Amplification of the resonance curves of Case 3 that is in the best agreement with the experimental results is also illustrated. Comparing with the test results, the resonance frequency and amplification obtained by Case 3 are underestimated and overestimated, while those calculated by Case C agreed better with the experimental ones. Finally, the soil property of Case C was adopted in the following investigations.

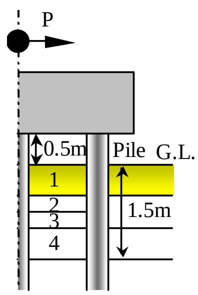

	Layer no.	Thickness (m)	Vs (m/s)	Damping (%)
case 3	1	0.5	50	5.0
	2	0.25	50	5.0
	3	0.25	80	3.0
	4	0.5	100	2.0
case 4	1	0.3	50	3.0
	2	0.3	80	3.0
	3	0.4	80	3.0
	4	0.5	100	2.0

Fig. 2 Predicted and modified analysis cases

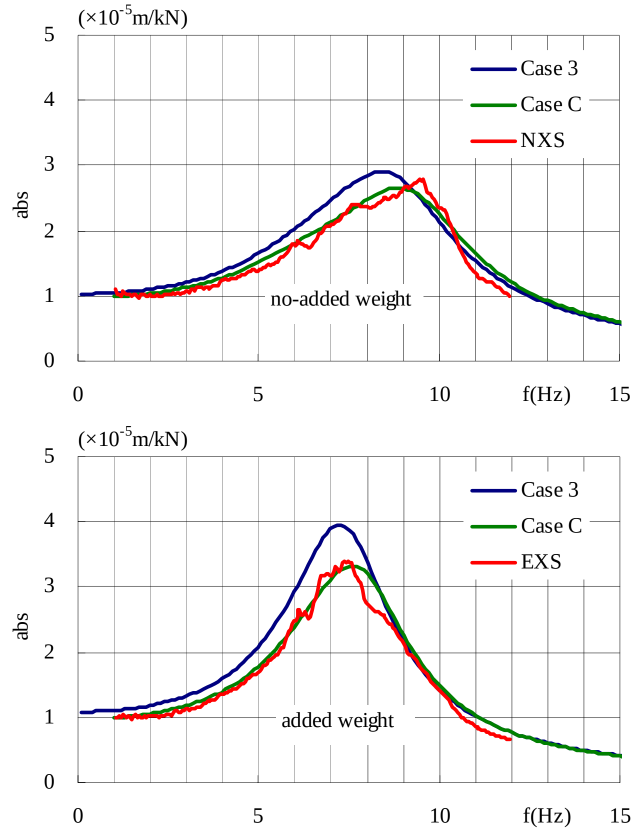

Fig. 3 Comparison of displacement resonance curves of each exciting force level at upper surface of foundation

Identification of impedance functions

Aggregated sway, rocking and coupled sway-rocking soil impedance functions estimated from the test results are identified with the impedance functions obtained by analyses. The impedance functions are calculated by the following procedure. A foundation is supposed to be massless and rigid. Sway and rocking displacements, due to the horizontal exciting force $Q = 1e^{i\omega t}$ and the moment force $M = 1e^{i\omega t}$ applying at the bottom of the foundation, are denoted as u_{f1}, θ_{f1} and u_{f2}, θ_{f2}, respectively. When both forces apply to a foundation simultaneously, the following equation is derived

$$\begin{Bmatrix} u_f \\ \theta_f \end{Bmatrix} = \begin{bmatrix} u_{f1} & u_{f2} \\ \theta_{f1} & \theta_{f2} \end{bmatrix} \begin{Bmatrix} Q \\ M \end{Bmatrix} \tag{1}$$

where u_f, θ_f are the sway and rocking displacements at the bottom of the foundation. The matrix of impedance functions $[K]$ can be written as

$$[K]=\begin{bmatrix} K_{HH} & K_{HR} \\ K_{RH} & K_{RR} \end{bmatrix}=\begin{bmatrix} u_{f1} & u_{f2} \\ \theta_{f1} & \theta_{f2} \end{bmatrix}^{-1} \quad , \quad K_{HR}=K_{RH} \tag{2}$$

Aggregated sway and rocking impedance functions are calculated by both measurement data with and without the added weight. The equation of motion utilized by the aggregated impedance functions is given as

$$\begin{Bmatrix} Q \\ M \end{Bmatrix}=\begin{bmatrix} K_H & 0 \\ 0 & K_R \end{bmatrix}\begin{Bmatrix} u_f \\ \theta_f \end{Bmatrix} \tag{3}$$

where m is a foundation mass including the added weight and J_0 is the moment of inertia at the center of gravity of the foundation. Then,

$$Q=P+\omega^2 m u_G \quad , \quad M=PH_P+\omega^2 m u_G H_G+\omega^2 J_0 \theta_f \tag{4}$$

Finally, aggregated sway and rocking impedance K_H, K_R in Fig. 4 are expressed as

$$K_H=\frac{P+\omega^2 m u_G}{u_f} \quad , \quad K_R=\frac{PH_P+\omega^2 m u_G H_G+\omega^2 J_0 \theta_f}{\theta_f} \tag{5}$$

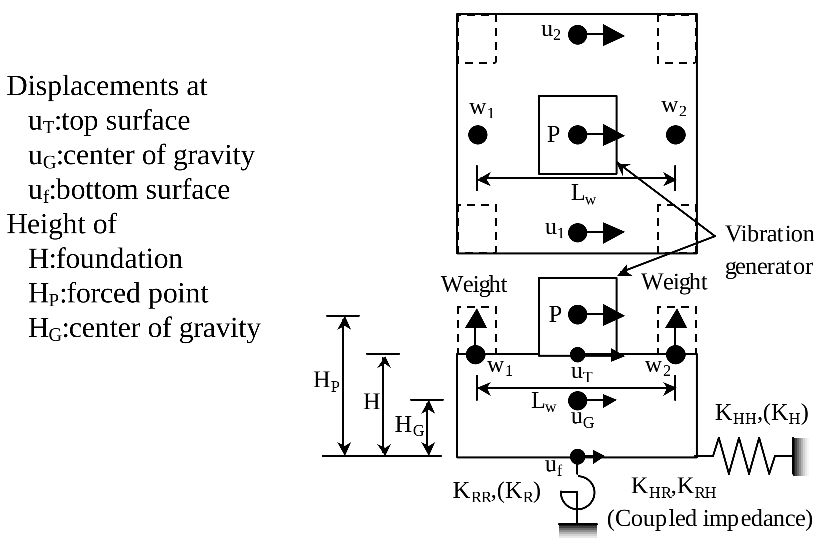

Fig. 4 Vibration generator and its foundation model

Using Eq. (5), the aggregated sway and rocking impedance functions including and excluding the added weight are estimated. Fig. 5 shows the sway and rocking impedance functions identified by the measure data and the functions simulated by the soil profile of Case C. Simulation results agree roughly with the identified ones. The identified impedance functions are in a good agreement with the simulation ones below 13 Hz, therefore the soil surrounding the foundation models is assumed to be linear. On the other hand, the equation of motion at the bottom of the foundation considering the coupled sway-rocking mode is given as follows.

$$\begin{Bmatrix} Q \\ M \end{Bmatrix} = \begin{bmatrix} K_{HH} & K_{HR} \\ K_{RH} & K_{RR} \end{bmatrix} \begin{Bmatrix} u_f \\ \theta_f \end{Bmatrix} \quad , \qquad K_{HR} = K_{RH} \tag{6}$$

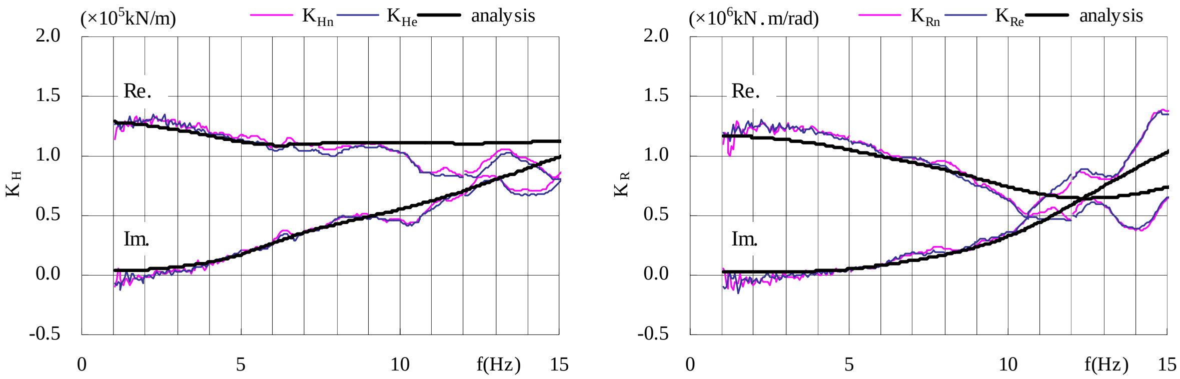

Fig. 5 Comparison of sway & rocking springs estimated by experiment and analysis

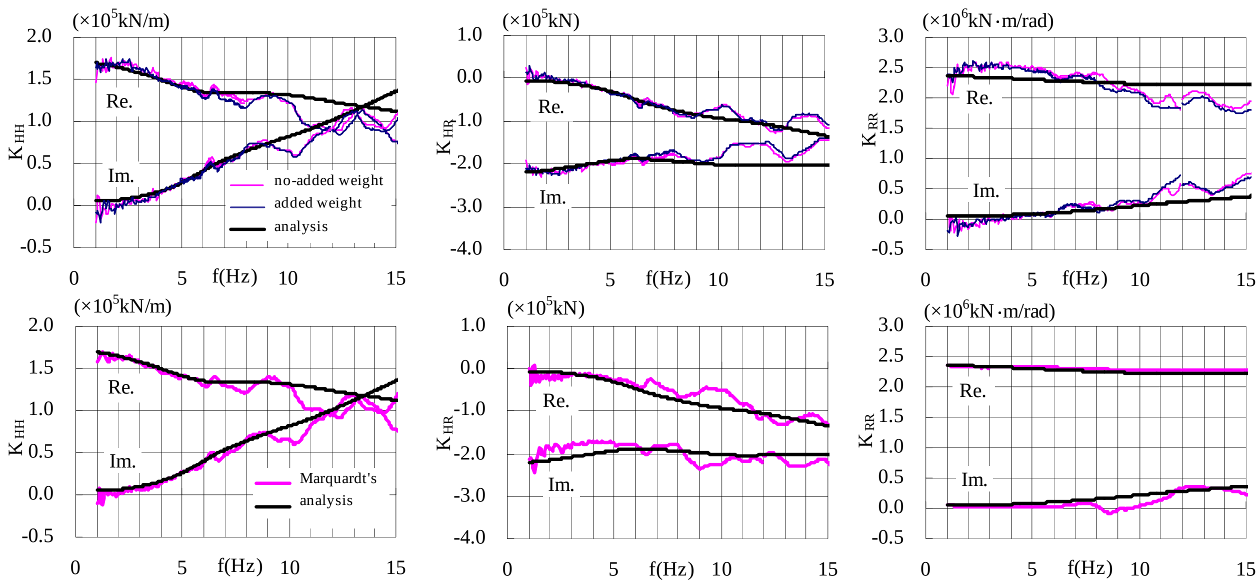

Fig. 6 Coupled sway & rocking impedance
(top: elimination method, bottom: Marquardt's method)

The coupled sway-rocking impedance functions are identified by both the Marquardt's method and the elimination method [6] that adopted the analysis solution derived by the thin layer formulation. In the latter method, the aggregated impedance at the start frequency is assumed to be an initial value, and convergence calculation is carried out. The convergence value is supposed to be the initial value at the next step, and the coupled impedance functions are identified at each frequency. The advantage of the Marquardt's method is that the coupled impedance functions are available by using the test results including and excluding the added weight even if no analytical solution is obtained. The coupled impedance functions identified by the elimination and Marquardt's method, and the functions simulated by the soil profile of Case C are plotted in Fig. 6. The elimination method can obtain the coupled impedance functions on both weight conditions, and little difference of the impedance functions including and excluding the added weight is seen as the same as the aggregated impedance functions. Comparing the differences of the coupled sway-rocking and rocking impedance functions in both methods, K_{HR}, K_{RR} are somewhat larger than the sway impedance function, K_{HH} .

DYNAMIC CHARACTERISTICS OF ADJACENT FOUNDATIONS

Procedure of flexible volume method

When an exciting force P_F is applied to a single foundation supported by piles, the equation of the motion of the pile-foundation system is given in the following forms:

$$\begin{bmatrix} K_{FF} & K_{FP} \\ K_{PF} & K_{PP}+S(i\omega) \end{bmatrix} \begin{bmatrix} u_F \\ u_P \end{bmatrix} = \begin{bmatrix} P_F \\ 0 \end{bmatrix} \tag{7}$$

where $K_{FF}, K_{FP}, K_{PF}, K_{PP}$ are sub-matrices of the dynamic stiffness of the pile-foundation system, $S(i\omega)$ is the dynamic impedance function of the pile-soil system calculated by the thin layer formulation, and u_F, u_P are the displacement vectors of the foundation and the piles. We considered multiple foundation models, three pile-supported foundations, a pile-embedded and an embedded foundation, as shown in Fig. 7. As for the single foundation, the equation of motion of the multiple heterogeneous foundation system is given by the following. In the following equation, the expression $(i\omega)$ will be omitted. The superscripts in this equation denote the number of foundations. The dynamic impedance matrices $[S^*_{FF}],[S^*_{FP}],([S^*_{PF}]),[S^*_{PP}]$ have a dynamic cross interaction effect on foundation-soil-foundation, foundation-soil-piles and piles-soil-piles, respectively.

$$\begin{bmatrix}
[K^1_{FF}] & [K^1_{FP}] & & & & & & & \\
 & [K^1_{PP}]+[S^{11}_{PP}] & & [S^{12}_{PP}] & & [S^{13}_{PP}] & [S^{14}_{PF}] & [S^{14}_{PP}] & [S^{15}_{PF}] \\
 & & [K^2_{FF}] & [K^2_{FP}] & & & & & \\
 & & & [K^2_{PP}]+[S^{22}_{PP}] & & [S^{23}_{PP}] & [S^{24}_{PF}] & [S^{24}_{PP}] & [S^{25}_{PP}] \\
 & & & & [K^3_{FF}] & [K^3_{FP}] & & & \\
 & & & & & [K^3_{PP}]+[S^{33}_{PP}] & [S^{34}_{PF}] & [S^{34}_{PP}] & [S^{35}_{PF}] \\
 & & sym. & & & & [K^4_{FF}]+[S^{44}_{FF}] & [K^4_{FP}]+[S^{44}_{FP}] & [S^{45}_{FF}] \\
 & & & & & & & [K^4_{PP}]+[S^{44}_{PP}] & [S^{45}_{PF}] \\
 & & & & & & & & [K^5_{FF}]+[S^{55}_{FF}]
\end{bmatrix}
\begin{bmatrix} \{u^1_F\} \\ \{u^1_P\} \\ \{u^2_F\} \\ \{u^2_P\} \\ \{u^3_F\} \\ \{u^3_P\} \\ \{u^4_F\} \\ \{u^4_P\} \\ \{u^5_F\} \end{bmatrix}
=
\begin{bmatrix} \{0\} \\ \{0\} \\ \{0\} \\ \{0\} \\ \{P^3_F\} \\ \{0\} \\ \{0\} \\ \{0\} \\ \{0\} \end{bmatrix} \tag{8}$$

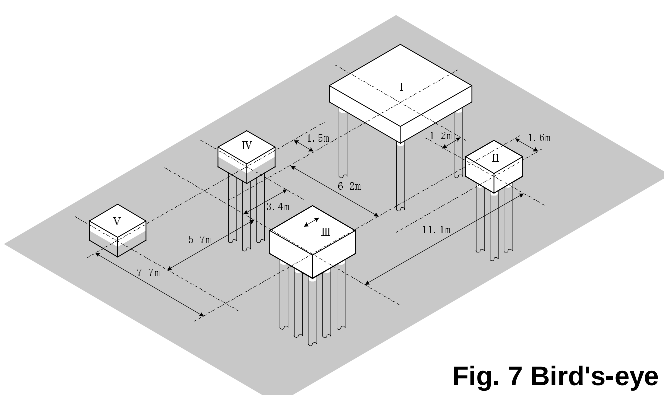

Fig. 7 Bird's-eye view of mock-up foundation models

These are the dynamic impedance functions of the multiple heterogeneous foundation system obtained by the solution of the thin layer approach. The diagonal terms of the matrix in Eq. (8) $[K^*_{**}]+[S^*_{**}]$ that are illustrated in Fig. 8 are described as follows. First, the soil impedance matrices related to the soil-piles and soil-foundations are calculated at nodal points distributed on the surface of the layers in the soil area where the foundations and piles will be installed. Then, the soil impedance matrix with excavation can be expressed by subtracting the stiffness and mass matrices of the foundations and piles made up of the soil property from the above impedance matrix. Finally, the total stiffness matrix of the foundations-piles-soil system is obtained by adding the stiffness and mass matrices of appropriated actual foundations and piles to the soil impedance matrix with excavation. The soil is modeled by thin layer elements, where nodal points corresponding to the soil, foundations and piles with three degrees of freedom are spatially distributed on the surface of thin-layers. Piles are modeled by the beam element taking account of the bending-shear type and that one of their nodes has six degrees of freedom. Foundations are treated as blocks modeled by hexagon elements.

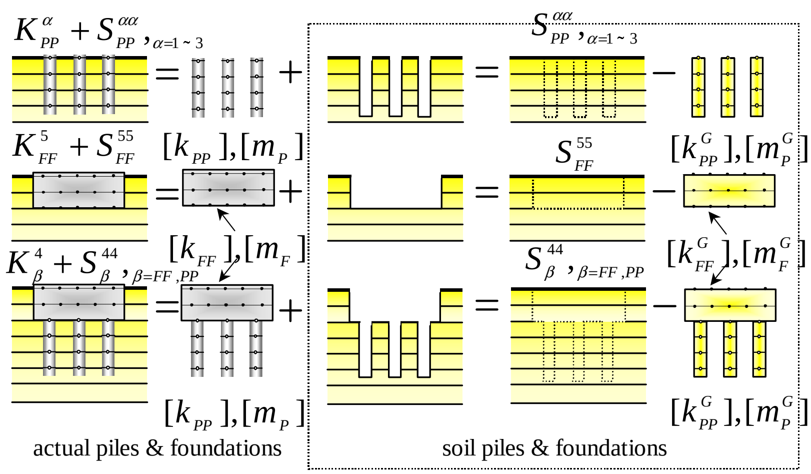

Fig. 8 Concept of Flexible Volume Method

Simulation analysis of forced vibration response

Five mock-up heterogeneous foundation models are arranged 3-dimensionally as in Fig. 7 to conduct simulation analyses of the forced vibration experiment. It assumes that the stress transmission between pile foundations (models I, II, III) and soil are only done by the piles themselves, while foundation V radiates stresses to the soil from its embedded parts. On the other hand, the interactions between foundation model IV and the soil are assumed to be between the piles and the embedded area except for the bottom of the foundation. Model profiles of the soil, pile and foundation for simulation analyses are shown in Tables 2, 3 and 4.

Table 2 Soil profile for simulation analysis

Thickness (m)	Mass density (ton/m^3)	Vs (m/s)	Poisson's ratio	Damping (%)
0.3	1.4	50	0.420	1.0
0.7	1.4	80	0.420	
0.5	1.4	100	0.420	
1.65	1.4	130	0.420	
3.8	1.5	150	0.488	
12.15	1.85	255	0.496	
6.90	1.85	350	0.476	
26.00	1.85	400	0.469	
-	1.85	400	0.469	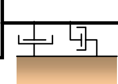

Table 3 Pile profile

Material	Steel	
Length	26.6	m
Diameter(D)	406.4	mm
Thickness	9.5	mm
Section area	118.5	cm^2
Mass per unit length	88.2	kg/m
Moment of inertia	2.334×10^4	cm^4
Young's modulus	2.06×10^7	N/cm^2

Table 4 Model profile

Model	Dimension (m)	Mass (ton)	Pile number	Pile space	Remarks
I	5×5×1	60	4	10D	
II	2×2×1.2	11.5	4	2.5D	
III	3×3×1.4	30.2	9	2.5D	
IV	2×2×1.2	11.5	4	2.5D	Embedded
V	2×2×1.2	11.5	None	-	Embedded raft

In the simulation analyses, the horizontal force 1 kN in the EW direction is applied to the center of gravity of the vibration generator where the height is 0.3 m from the top surface of the foundation. Displacement resonance curves of the five mock-up foundations in terms of NXS and simulation models are illustrated in Fig. 9. Fig. 9 also shows the simulation results of foundation III, which only exists in the analysis and is excited by the vibration generator.

The multiple analysis models simulate peaks at 8 and 9 Hz of the displacement resonance curves of the mock-up foundations, while the single one obtain a peak at 9 Hz. It seems that the peak at 9 Hz, which appears in the results of the adjacent simulation models except for foundation I, is resonated by the excited foundation. The amplifications of the simulation results of foundation IV and V are smaller than those of other foundations because of the embedment effect. According to the corresponding paper [7], the resonance frequency of foundation I is lower than that of the excited foundation III because its weight and pile spacing ratio is heavier and bigger than that of other foundations.

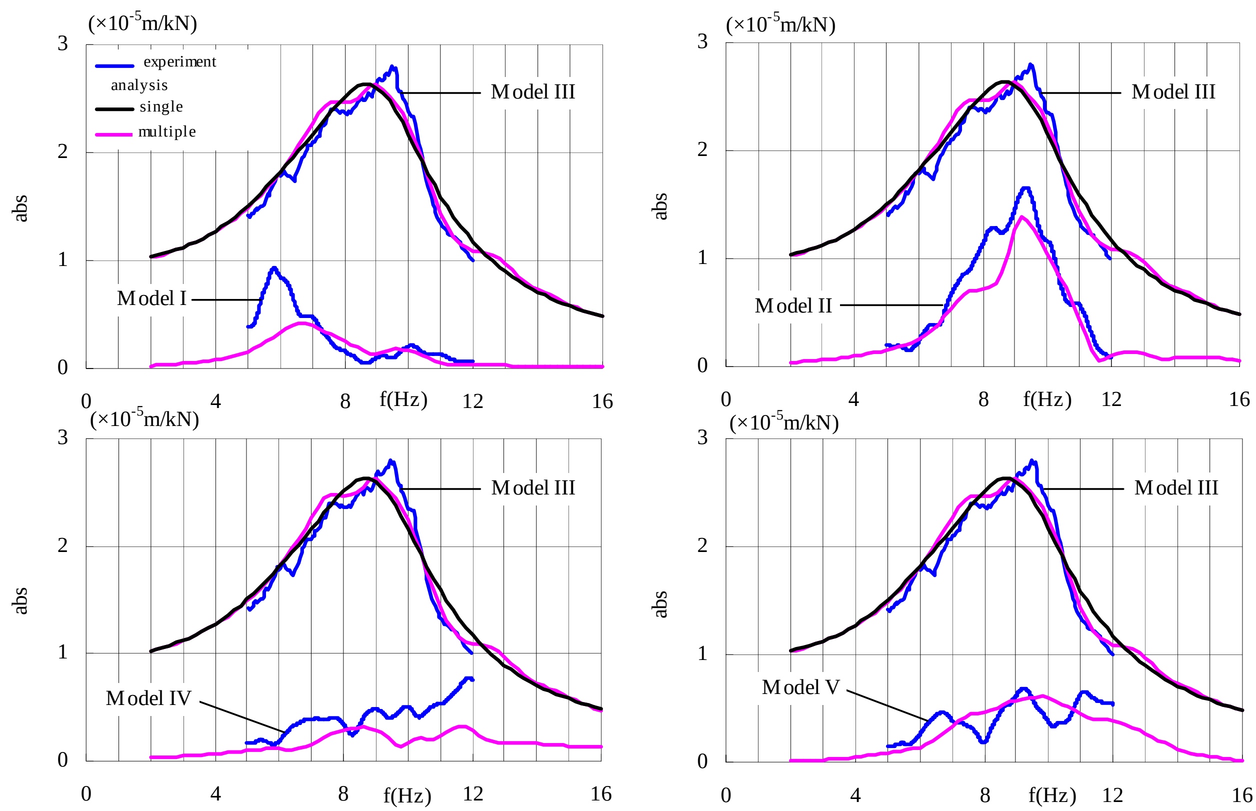

Fig. 9 Comparison of displacement resonance curves at each foundation (experiment and analysis)

The displacement resonance curves of foundation I from the test and simulation display the peaks at about 6 Hz independent of oscillation of foundation III. Another simulation analysis of the multiple foundations excluding foundation I is carried out to confirm that the presence of the massive foundation I affects the behavior of other adjacent foundations. The displacement resonance curves of foundations II and III in the multiple foundation models with and without foundation I are shown in Fig. 10. The result of foundation III in multiple models without foundation I has no peak at 8 Hz and is close to that of the single simulation model. It seems that the resonance curves of the multiple foundations are affected by foundation I as well as the decrease of the peak of the result of foundation II.

Steady state harmonic analysis

Utilizing the multiple heterogeneous foundation models in the forced vibration test analyses, earthquake response analysis is also carried out. The transfer functions of the plural foundation models to the steady state harmonic incident wave defined at the bottom of the analysis soil model are illustrated in Fig. 11. Thin solid lines in Fig. 11 represent the transfer functions of each foundation assumed to be a single foundation. It is found that response of the massive foundation I is appreciably bigger than that of the vibration test and transfer function of foundation II in the multiple foundation models is greater than that of the single foundation II.

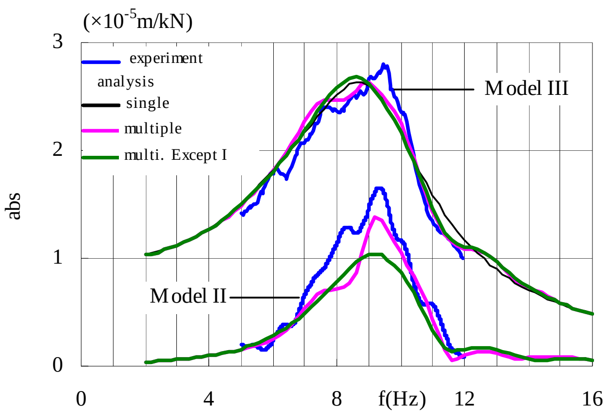

Fig. 10 Comparison of displacement resonance curves of model II&III including and excluding model I

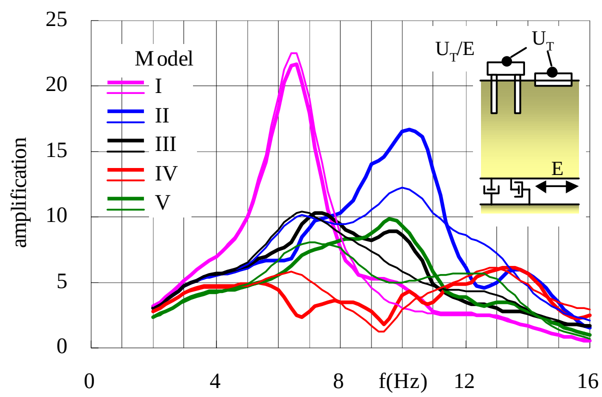

Fig. 11 Transfer functions of multiple and single foundation models subjected to steady state harmonic incident wave (heavy line: multiple, thin line: single)

Earthquake observation of multiple foundations

Figure 12 shows a plan view of the experiment site of five mock-up pile foundations. Accelerometers have been placed on the multiple foundations and inserted into ground holes. The accelerometers have measuring components of x, y and z directions. The installed depths of the accelerometers are at G.L.-3.5m,-6.5m,-25m. Figures 13 and 14 show the transfer functions of a point at the upper side of foundations I, II and III to G.L.-25m at ground point B in the EW and NS directions. Transfer functions of G.L.-3.5m to G.L.-25m at ground point B are also illustrated in both figures. These transfer functions are calculated by average of three earthquake records that are medium and small in magnitude. According to both of the transfer functions it seems that the predominant frequencies of the site are 4Hz and 12Hz. The frequency behaviors of both transfer functions are quite different during the 5Hz to 10Hz. The cross interaction among the foundations might affect the transfer functions of the foundation models and the ground points. Now, the equation of motion of the plural foundation system including observation point B for earthquake response is given by the following:

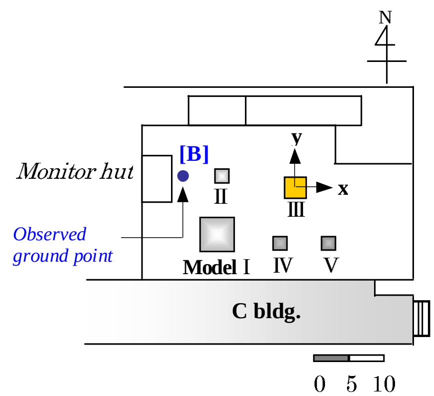

Fig. 12 Illustration of accelerations at point B

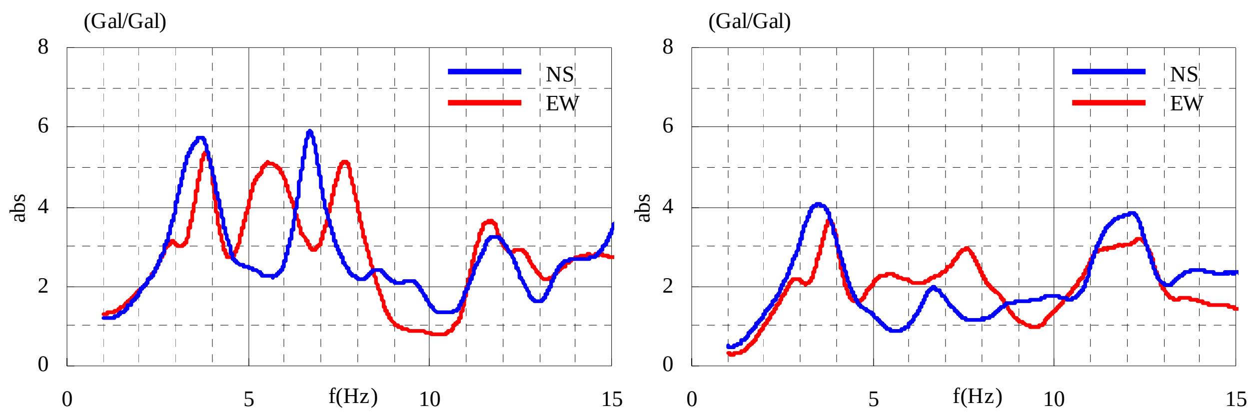

Fig. 13 Comparison of transfer functions of G.L.-3.5 m and -6.5 m to G.L.-25 m at point B

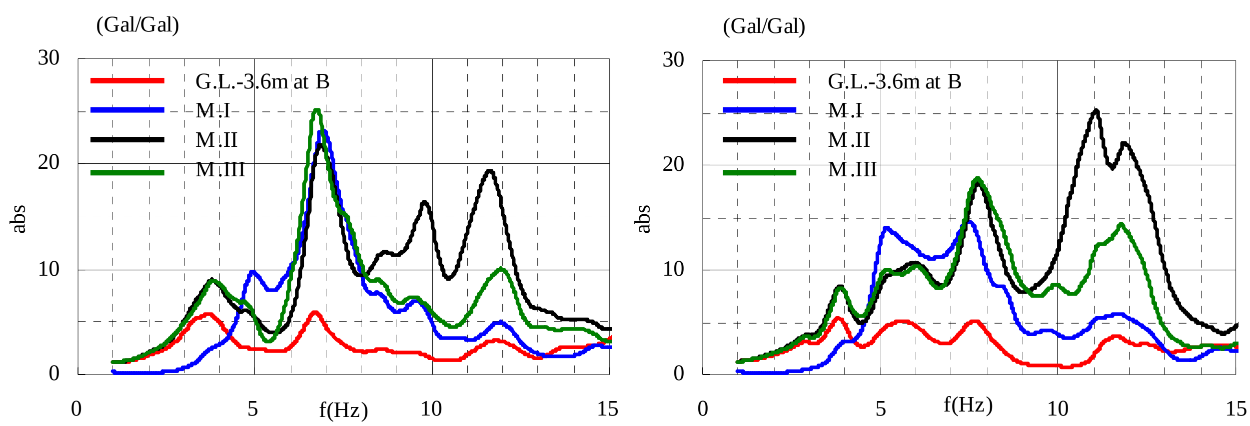

Fig. 14 Comparison of transfer functions of a point at the upper surface of foundations I, II and III to G.L.-25 m at point B (left : NS direction, right : EW direction)

$$
\begin{bmatrix}
[K_{FF}^{1}] & [K_{FP}^{1}] & & & & & & & & \\
 & [K_{PP}^{1}]+[S_{PP}^{11}] & & [S_{PP}^{12}] & & [S_{PP}^{13}] & [S_{PF}^{14}] & [S_{PP}^{14}] & [S_{PF}^{15}] & [S_{PS}^{16}] \\
 & & [K_{FF}^{2}] & [K_{FP}^{2}] & & & & & & \\
 & & & [K_{PP}^{2}]+[S_{PP}^{22}] & & [S_{PP}^{23}] & [S_{PF}^{24}] & [S_{PP}^{24}] & [S_{PP}^{25}] & [S_{PS}^{26}] \\
 & & & & [K_{FF}^{3}] & [K_{FP}^{3}] & & & & \\
 & & & & & [K_{PP}^{3}]+[S_{PP}^{33}] & [S_{PF}^{34}] & [S_{PP}^{34}] & [S_{PF}^{35}] & [S_{PS}^{36}] \\
 & & & & & & [K_{FF}^{4}]+[S_{FF}^{44}] & [K_{FP}^{4}]+[S_{FP}^{44}] & [S_{FF}^{45}] & [S_{FS}^{46}] \\
 & & sym. & & & & & [K_{PP}^{4}]+[S_{PP}^{44}] & [S_{PF}^{45}] & [S_{PS}^{46}] \\
 & & & & & & & & [K_{FF}^{5}]+[S_{FF}^{55}] & [S_{FS}^{56}] \\
 & & & & & & & & & [S_{SS}^{66}]
\end{bmatrix}
\begin{Bmatrix}
\{u_F^1\} \\ \{u_P^1\} \\ \{u_F^2\} \\ \{u_P^2\} \\ \{u_F^3\} \\ \{u_P^3\} \\ \{u_F^4\} \\ \{u_P^4\} \\ \{u_F^5\} \\ \{u_S^6\}
\end{Bmatrix}
$$

$$
=\begin{bmatrix}
 & & & & & & & & & \\
 & [S_{PP}^{11}] & & [S_{PP}^{12}] & & [S_{PP}^{13}] & [S_{PF}^{14}] & [S_{PP}^{14}] & [S_{PF}^{15}] & [S_{PS}^{16}] \\
 & & & & & & & & & \\
 & & & [S_{PP}^{22}] & & [S_{PP}^{23}] & [S_{PF}^{24}] & [S_{PP}^{24}] & [S_{PP}^{25}] & [S_{PS}^{26}] \\
 & & & & & & & & & \\
 & & & & & [S_{PP}^{33}] & [S_{PF}^{34}] & [S_{PP}^{34}] & [S_{PF}^{35}] & [S_{PS}^{36}] \\
 & & & & & & [S_{FF}^{44}] & [S_{FP}^{44}] & [S_{FF}^{45}] & [S_{FS}^{46}] \\
 & sym. & & & & & & [S_{PP}^{44}] & [S_{PF}^{45}] & [S_{PS}^{46}] \\
 & & & & & & & & [S_{FF}^{55}] & [S_{FS}^{56}] \\
 & & & & & & & & & [S_{SS}^{66}]
\end{bmatrix}
\begin{Bmatrix}
\{0\} \\ \{g_P^1\} \\ \{0\} \\ \{g_P^2\} \\ \{0\} \\ \{g_P^3\} \\ \{g_F^4\} \\ \{g_P^4\} \\ \{g_F^5\} \\ \{g_S^6\}
\end{Bmatrix}
=\begin{Bmatrix}
\{0\} \\ \{F_P^1\} \\ \{0\} \\ \{F_P^2\} \\ \{0\} \\ \{F_P^3\} \\ \{F_F^4\} \\ \{F_P^4\} \\ \{F_F^5\} \\ \{F_S^6\}
\end{Bmatrix}
\qquad (9)
$$

where $\{g_*^*\}$, $\{F_*^*\}$ are the displacement vectors of the earthquake input motion and the driving force taking into account the cross interaction effects. The superscript denotes the number of foundations and point B, while subscripts P, F and S represent piles, foundations and point B, respectively. The displacements of the earthquake input motion and the driving force consist of three components x, y and z. $[S_{SS}^{66}]$ is the dynamic impedance matrix of point B itself, and $[S_{*S}^{*6}]$ means the coupled impedance functions between point B and the piles or foundations. When multiple foundation models are subjected to an arbitrary earthquake input motion, all of the foundations generate 6 component responses, and three responses of x, y and z directions are obtained at point B. In the simulation analysis, it is necessary for the foundation models and point B to superpose responses caused by three components of earthquake input motions to compare earthquake records.

Earthquake analysis procedure for multiple foundations

First an analysis of the steady state harmonic incident wave defined at the bottom of the soil model has been carried out for each x (EW), y (NS) and z direction, and transfer functions of foundations and ground points were obtained as shown in Fig.15. The transfer function of arbitrary point i in direction L to the steady state harmonic incident wave in direction M defined at the bottom of the soil model is expressed as $H^{i(L)j(M)}(i\omega)$. Displacement of point i in direction L is given by

$$
U^{i(L)}(i\omega) = \sum_{L,M=x,y,z} H^{i(L)j(M)}(i\omega)\cdot U_g^{j(M)}(i\omega) \qquad (10)
$$

where $U_g^{j(M)}(i\omega)$ is an earthquake spectrum in direction M defined at the bottom of the soil model and is an unknown quantity. On the other hand, $H_K^{i(L)j(M)}(i\omega)$ is a known quantity and is estimated by analysis. $U^{i(L)}(i\omega)$ is also a known quantity and is obtained by the earthquake records. Therefore, the unknown quantity $U_g^{j(M)}(i\omega)$ can be calculated at each observation point i. For a single foundation, the term of $H_K^{i(L)j(M)}(i\omega)\ (L \neq M)$ in equation (10) can be neglected. For multiple foundations, we have to take the term of $H_K^{i(L)j(M)}(i\omega)\ (L \neq M)$ into consideration to estimate $U_g^{j(M)}(i\omega)$. Control motion $U_g^{j(M)}(i\omega)$ is defined by the least-squares method or by arbitrary observation points. Here, the latter is adopted.

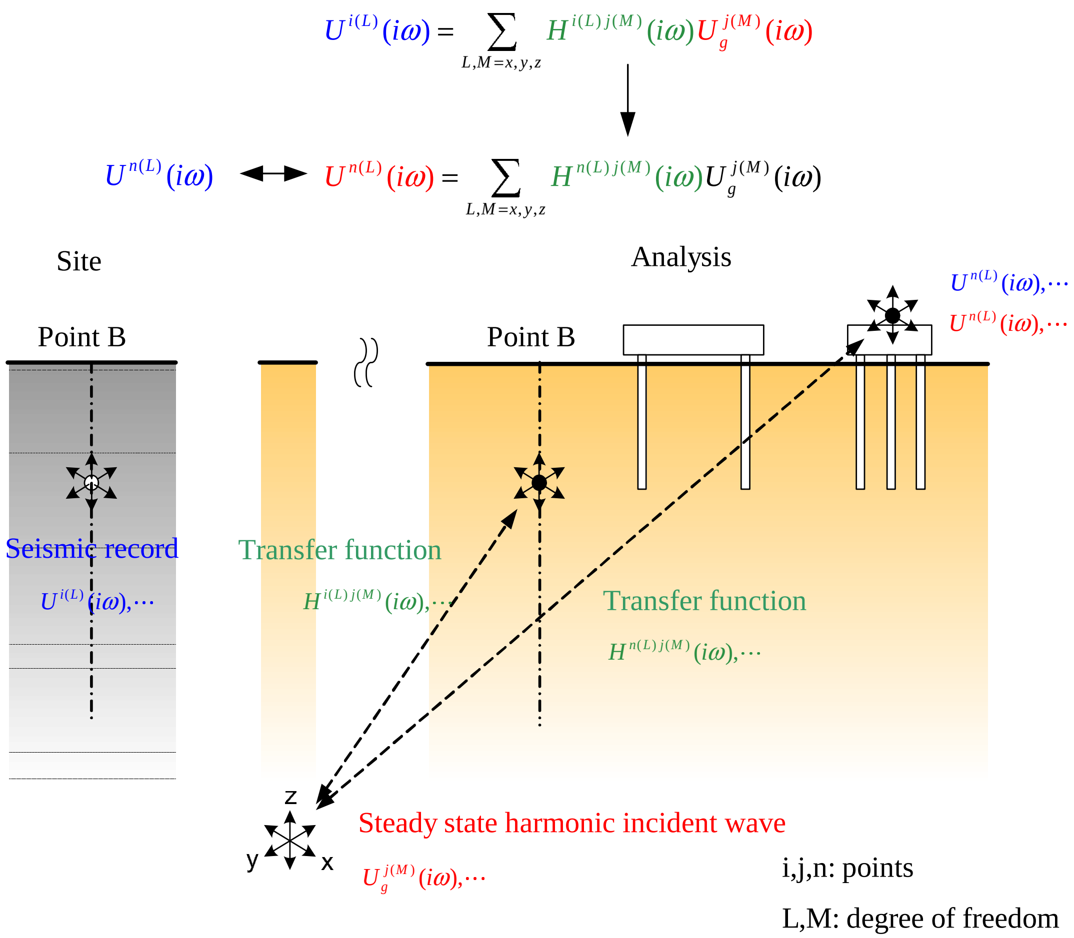

Fig. 15 Outline of calculating transfer functions of foundations and ground points

Comparison with records and analysis results

Figure 16 and 17 show the comparison of the acceleration transfer functions of a point at the upper side of foundations I, II and III to G.L.-25m at ground point B. The red line represents the earthquake record and the blue and green line has taken into account the result and neglected the cross interaction, respectively. In the NS direction, the analysis results agree well with the earthquake records. The result that has taken the cross interaction into consideration expresses the peak at 10Hz corresponding with the predominant frequencies of foundations II and III. The transfer functions of the observation records have peaks at 5Hz and 8Hz in the EW direction. On the other hand, the peak frequency of the analysis result is 6.5Hz; it does not agree with the observation records. The difference in the EW direction might be caused by soil nonlinearity or the existence of structures near the site; more detailed examine is required. The acceleration transfer functions of G.L.-3.5m to G.L.-25m at ground point B by analysis are compared with those of the earthquake records in Figure 18. The analysis transfer function of the ground points in the NS direction is also in good agreement with that of the earthquake records.

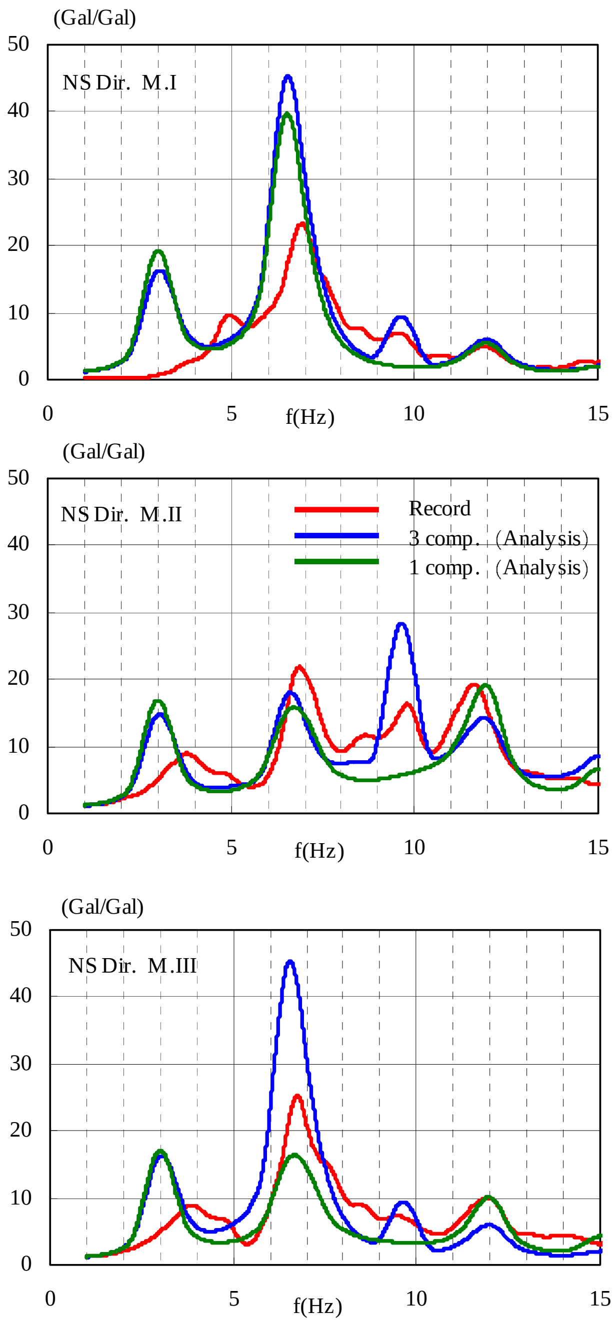

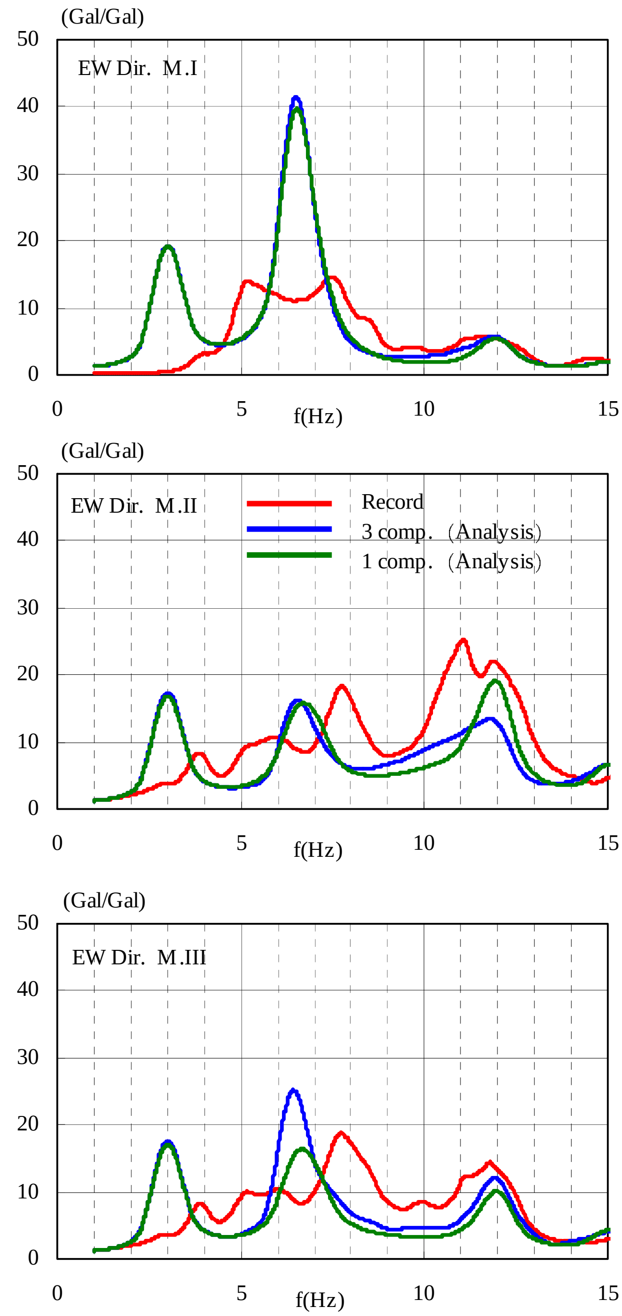

Fig. 16 Comparison of transfer functions of a point at the upper surface of foundations I, II and III to G.L.-25 m at point B (Seismic records vs Analysis NS direction)

Fig. 17 Comparison of transfer functions of a point at the upper surface of foundations I, II and III to G.L.-25 m at point B (Seismic records vs Analysis EW direction)

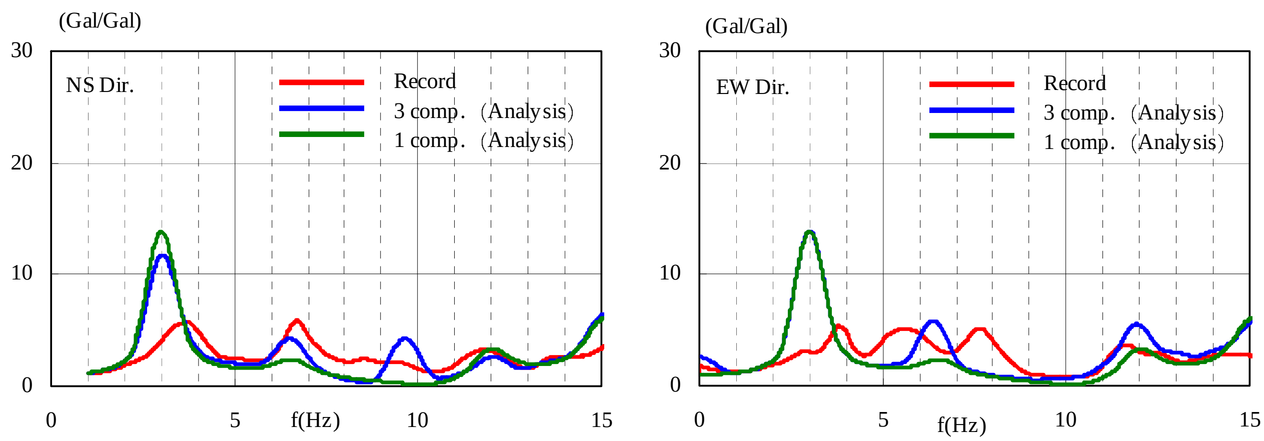

Fig. 18 Comparison of transfer functions of G.L.-3.5m to G.L.-25 m at point B (Seismic records vs Analysis NS & EW direction)

CONCLUSIONS

From the experimental and analytical results, the cross interaction among multiple foundation models is recognized. It is confirmed that the frequency behavior of the foundation fluctuated by a vibration generator affects adjacent foundations, and massive foundations affect the foundation with the vibration generator. It is suggested that the cross interaction among multiple foundations affects earthquake responses recorded at foundations and ground points. The analysis procedure that superposes response derived by three components of earthquake input motions to compare with the seismic records is proposed. It is found that the analysis results estimated by the present procedure agree well with the observation records.

ACKNOWLEDGEMENTS

This research was conducted as a part of the Academically Promoted Frontier Research Program on "Sustainable City Based on Environment Preservation and Disaster Prevention " at Nihon University, College of Science and Technology (Head Investigator: Prof. Ohtsu, I.) under a grant from the Ministry of Education, Science, Sports and Culture, Japan. The research was also partially supported by Grant-in-Aid for Science Research (B), 15360303, 2003, the Ministry of Education, Science, Sports and Culture. Furthermore, the authors wish to express their appreciation to Prof. Hanada, K., Prof. Adachi, H. and Associate Prof. Suzumura, J. of Nihon University, for their insightful suggestions and discussions throughout the tests.

REFERENCES

1. Tamori, S., Iiba, M. and Kitagawa, Y. "Dynamic Response Analysis of Soil-Pile-Building Interaction System in Large Strain Level of Soils." Proceedings of 12th World Conference on Earthquake Engineering, Auckland, New Zealand. Paper 1381. 2000.
2. Kontani, O., Saito, H., Tanaka, H., Kobayashi, Y., Fujiwara, K., Miyamoto, Y. and Suzuki, A. "Vibration Tests on Pile-Group Foundations using Large-Scale Blast Excitation." Transactions of the 17th International Conference on Structural Mechanics in Reactor Technology, Prague, Czech Republic. Paper # K12-3. 2003.

3. Mori, M. and Hasegawa, M. “Seismic Response Analysis of Pile-Supported Buildings Considering Material Nonlinearity and Pile-Soil Separation.” Proceedings of 12th World Conference on Earthquake Engineering, Auckland, New Zealand. Paper 1774. 2000.
4. Koyama, K., Sunasaka, Y., Morioka, Y. and Miyamoto, Y. “Seismic Safety Evaluation of An Existing Tank Supported by Piles in Liquefiable Ground.” Proceedings of 12th World Conference on Earthquake Engineering, Auckland, New Zealand. Paper 0947. 2000.
5. Shimomura, Y., Oshima, K., Kondo, R., Nakanishi, M. and Adachi, H. “A fundamental study on dynamic cross interaction of adjacent structures supported on pile foundations.” Transactions. of the 16 th International Conference on Structural Mechanics in Reactor Technology, NC, USA. Paper #1518. 2001.
6. Hasegawa, M and Adachi, H. “Inverse problem of experimental impedance functions based on forced vibration tests of a rigid block.” Journal of Structural and Construction Engineering (Transactions of Architectural Institute of Japan). No.492, pp.47-52, (in Japanese), 1997.
7. Shimomura, Y., Ikeda, Y., Ogushi, Y., Nakamura, M. and Arai, T. “Aging Effects on Dynamic Soil Springs of Pile Foundations Based on Forced Vibration Tests.” Proceedings of 13th World Conference on Earthquake Engineering, Vancouver, B.C., Canada. Paper 2187. 2004.